CHAPTER-VII

SMALL STRAIN SHEAR MODULUS OF UNTREATED AND TREATED SOIL AND CORRELATION STUDIES

7.1 INTRODUCTION

The bender element (BE) test is a widely used approach to measure the small-strain shear modulus (G_{max}) in geomaterials. G_{max} is a crucial soil parameter that aids in understanding the elastic behaviour of the soil and assessing its reaction to dynamic loads, such as traffic loads, earthquakes, and machine vibrations (Yamashita et al. 2009). The identification of non-linear behaviour has led to the development of a number of techniques to assess and better understand the dynamic response and particulate nature of soils. One such technique is the measurement of seismic waves, which allows for the study of the nature of the soil without compromising structural equilibrium, fabric, or intrinsic mechanical properties (Fam and Santamarina 1995). One of the key factors in the construction of machine foundations and buildings in earthquake-prone regions is the shear wave velocity. In addition, the shear wave velocity is employed to investigate the clay soil consolidation process and also to identify the quality of soil samples (Fam and Santamarina 1997; Landon et al. 2007). The importance of soil stiffness, which is commonly expressed by shear modulus, in both static and dynamic behaviour at low shear strain levels has raised interest in laboratory techniques for detecting stiffness at low strains. The most popular method for determining shear wave velocity and, consequently, shear modulus is to employ bender elements, which are small piezoceramic devices that can produce and detect waves in soil (Xu et al. 2014).

Nevertheless, a static assessment would not be sufficient for the safe building of structures given the current seismic activity. Consequently, it is important to examine the behaviour of the material or conduct a ground response analysis under dynamic condition; for this, in addition to dynamic properties, the normalised shear modulus (G/G_{max}) is required. This chapter therefore examines the small-strain shear modulus for both treated and untreated soil under different experimental conditions and the same has been used for the development of normalised shear modulus (G/G_{max}) for both treated and untreated soil.

7.2 ASSESSMENT OF NANO-SiO_2 ON SMALL-STRAIN SHEAR MODULUS

The variation of small-strain shear modulus (G_{max}) against 1% Nano-SiO_2 content for the curing ages of 1 day, 7 days, and 28 days with different confining pressure of 50 kPa, 100 kPa, and 150 kPa is presented in Fig.7.1 (a) and Fig.7.1 (b). As the confining pressure and curing times increased, a substantial increment in the shear wave velocity (V_s) was observed; thereby, G_{max} was increased. The shear modulus increased to 2.41 times higher than the untreated soil during 28 days curing period. Stabilization results in a stiffer and denser soil matrix; the treated soil has a greater V_s value than the parent soil. The void spaces between the soil particles were also compressed as the confining pressure increased, which led to an increase in the compactness of the sample. The rise in G_{max} was caused by a greater degree of compactness (Lang et al. 2020). The G_{max} of the clay soil treated with Nano-SiO_2 was 3.2 times higher than the untreated soil at a small-strain level (Thomas and Rangaswamy 2022). With the rise in fly ash content, the shear wave velocity of clay soil was raised (Kang and Bate 2016, Petcherdchoo et al. 2023). The geopolymer-stabilized soil sample exhibited a V_s value of more than 500 m/s, the geotechnical engineering limit value for the stiff ground. This result demonstrated the viability and superiority of using geopolymer for improving the strength of the soft clay (Wu et al. 2021).

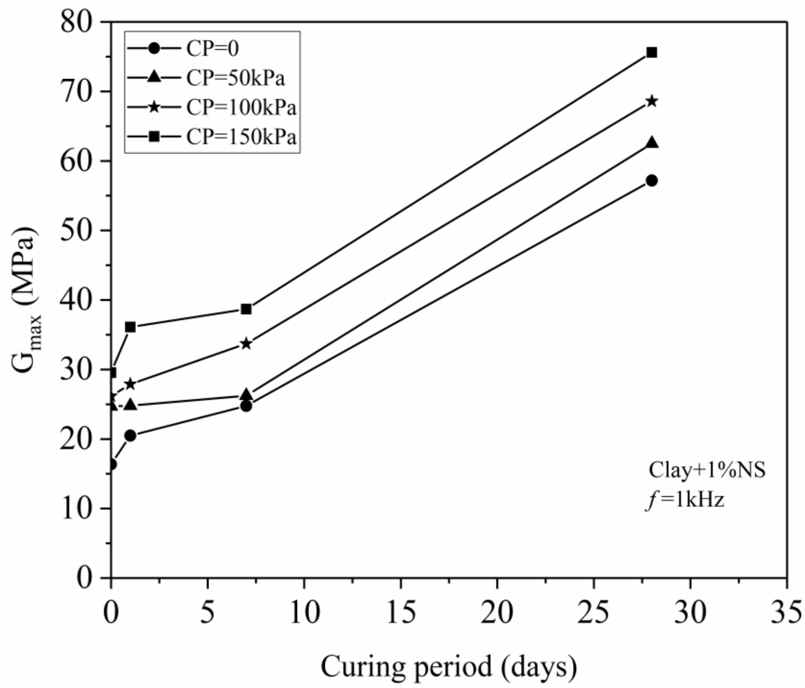

(a)

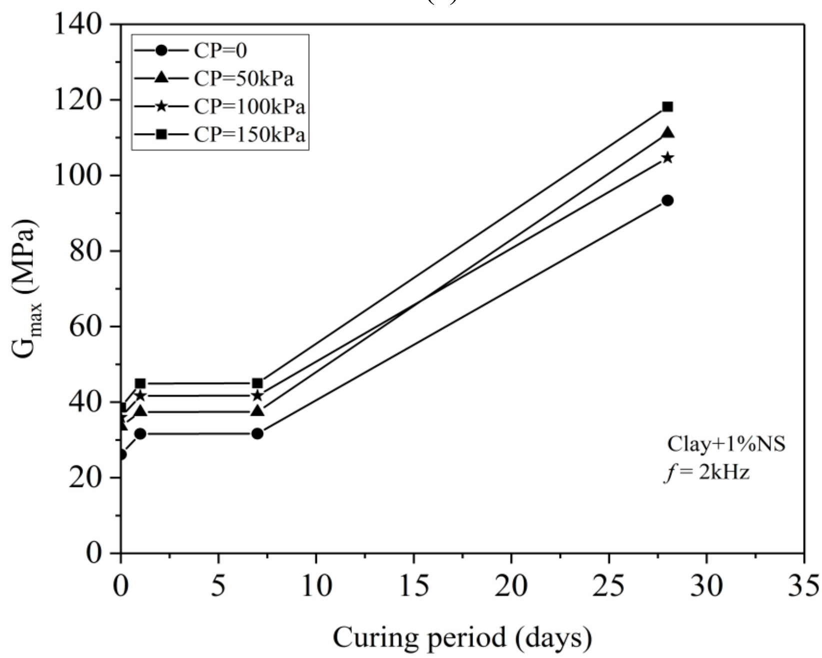

(b)

Fig. 7.1. Variation of G_{max} with nano-SiO_2 content for variable curing periods (a) Clay+ 1%NS, *f*=1kHz, and (b) Clay+1%NS, *f* =2kHz.

7.3 ASSESSMENT OF THE OPTIMISED NANO-SiO_2 AND FLY ASH ON SMALL-STRAIN SHEAR MODULUS

The results of G_{max} with various contents of fly ash (10%, 20%, and 30%) and 1% Nano-SiO_2 for the curing ages of 1 day, 7 days, and 28 days are illustrated in Fig.7.2 (a) and (b); Fig.7.3 (c), d); Fig. 7.4 (e) and (f). The figure shows that for both the input frequency of 1 kHz and 2 kHz, the shear modulus (G_{max}) was increased with the curing periods. Fig.7.5 (a) and (b); Fig. 7.6 (c), (d); Fig.7.7 (e) and (f) depicts the variation of G_{max} with different percentages of fly ash and 1% of Nano-SiO_2 at various confining pressures. The results of V_s and G_{max} variation under various confining pressures are listed in Table 7.1. The maximum values of the shear wave velocity (V_s) and, thereby, G_{max} of the soil matrix were achieved with 1% of Nano-SiO_2 and 20% of fly ash. In the presence of water, the cementitious and pozzolanic interactions between the particles and binding agents filled the empty spaces with the cementitious gel. They created a denser soil matrix, which could increase the shear wave velocity (Thomas and Rangaswamy 2020). The bender element test results show good agreement as the treated soil matrix stiffens over the curing days (Bahmani et al. 2014). The stiffness properties of the silty clay can be significantly improved by mixing 5% cement with 30% fly ash as a stabilizer rather than 15% cement alone (Lang et al. 2020).

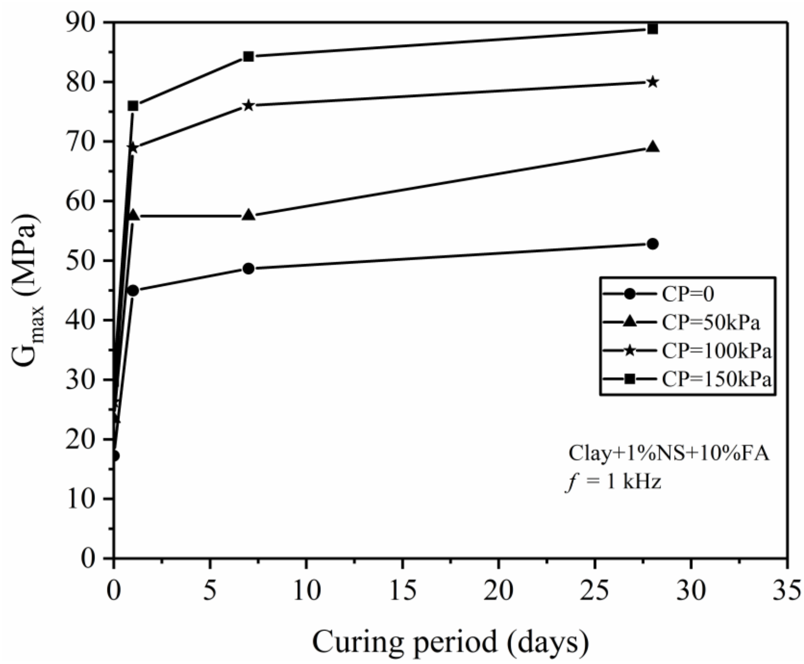

(a)

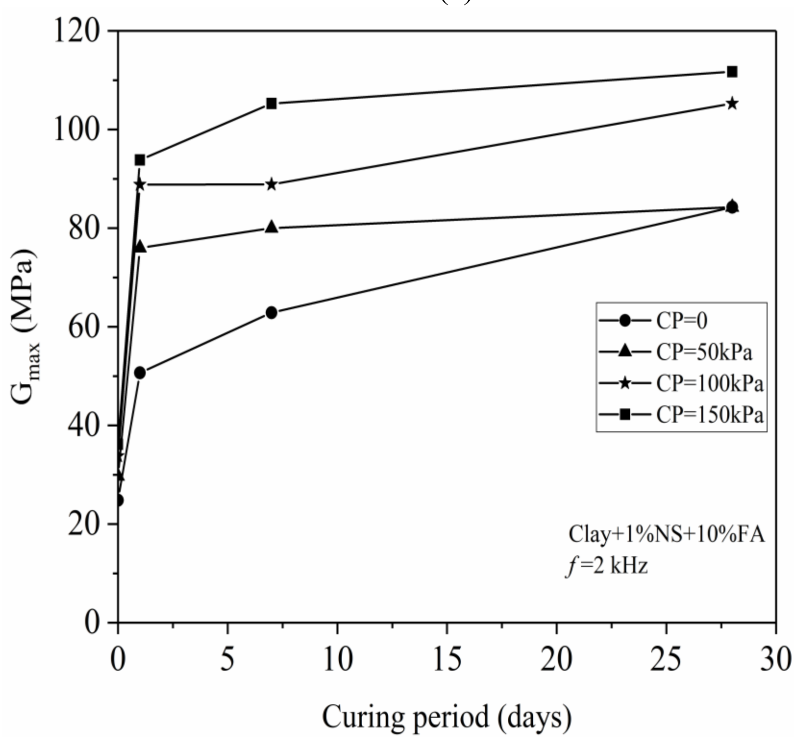

(b)

Fig. 7.2. Variation of G_{max} with nano-SiO_2 content for variable curing periods (a) Clay+1%NS+10%FA, f =1kHz, (b) Clay + 1% NS + 10%FA, f = 2kHz.

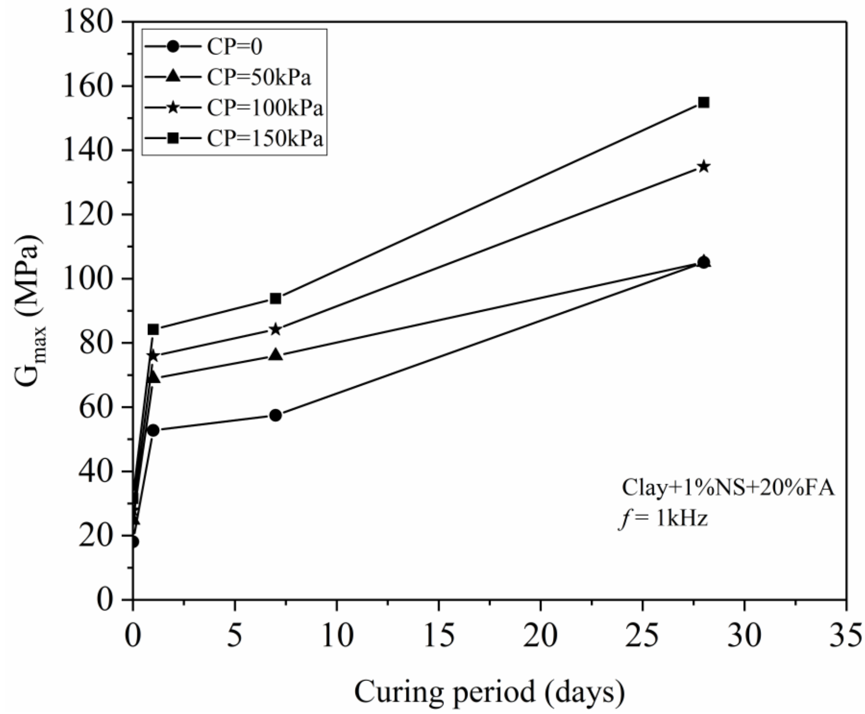

(c)

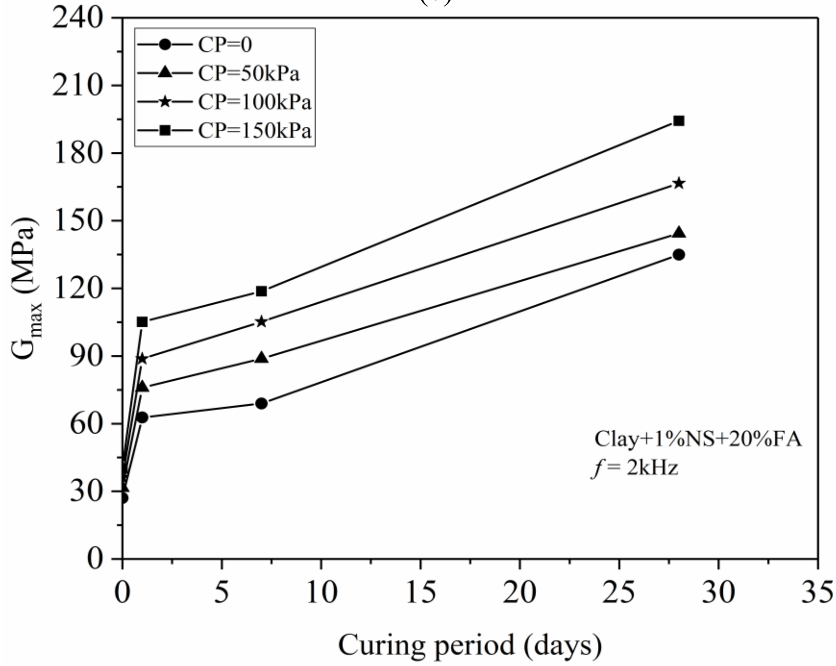

(d)

Fig. 7.3. Variation of G_{max} with nano-SiO_2 content for variable curing periods (c) Clay+1%NS+20%FA, *f*=1kHz, (d) Clay+1%NS+20%FA, *f*=2kHz.

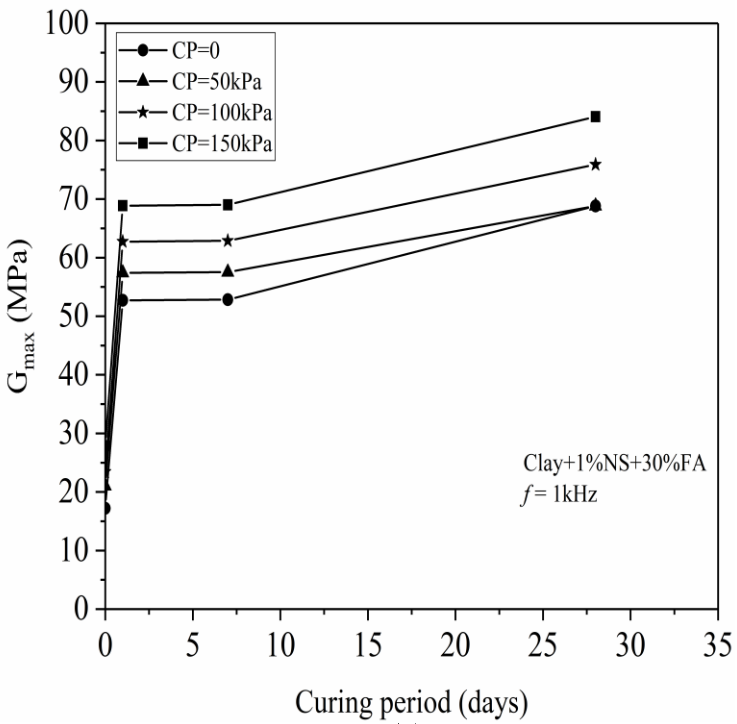

(e)

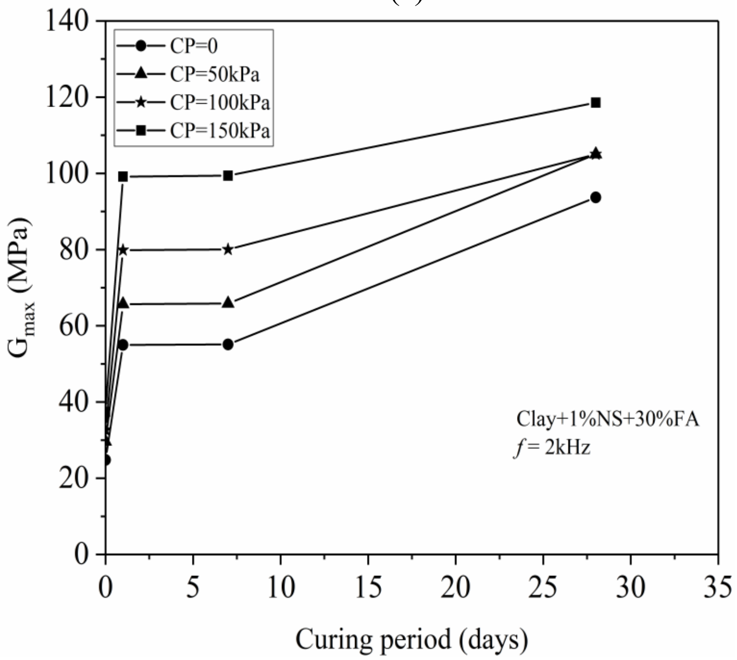

(f)

Fig. 7.4. Variation of G_{max} with nano-SiO_2 content for variable curing periods (e) Clay+1%NS+30%FA, *f*=1kHz, and (f) Clay+1%NS+30%FA, *f*=2kHz.

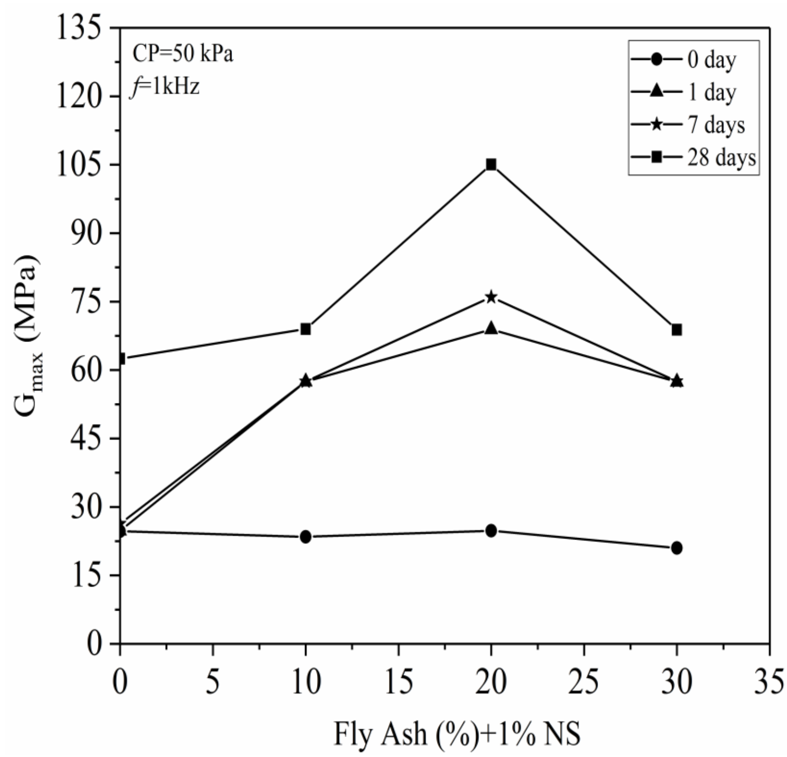

(a)

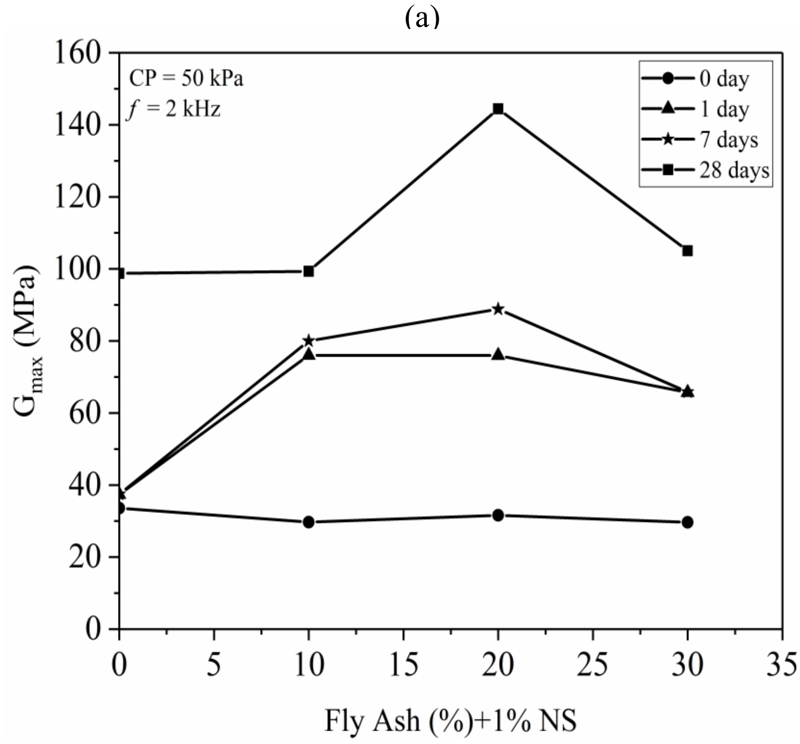

(b)

Fig. 7.5. Variation of G_{max} with fly ash and 1% Nano-SiO_2 (NS) content for variable curing periods (a) CP=50kPa, *f*=1kHz, (b) CP=50kPa, *f*=2kHz.

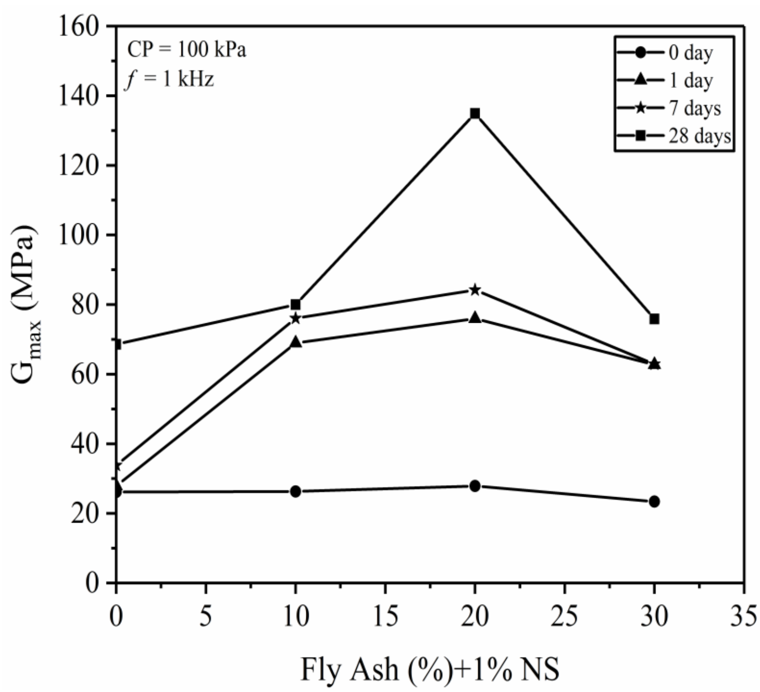

(c)

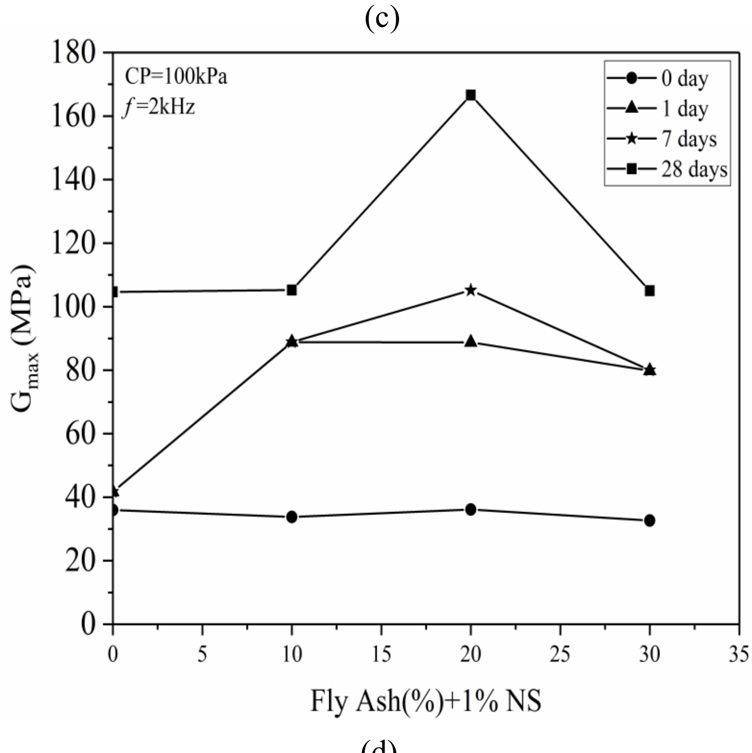

(d)

Fig. 7.6. Variation of G_{max} with fly ash and 1% Nano-SiO_2 (NS) content for variable (c) CP=100kPa, *f*=1kHz, (d) CP=100kPa, *f*=2kPa.

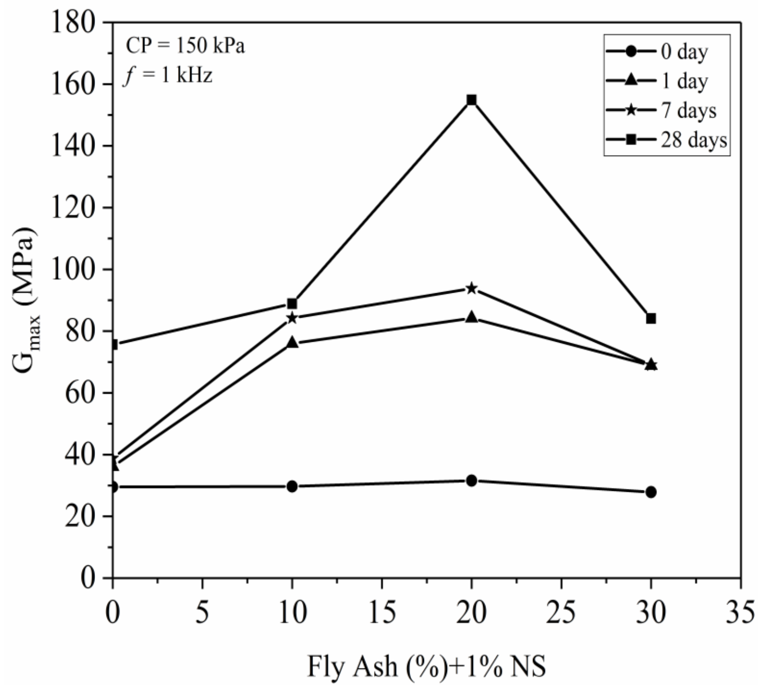

(e)

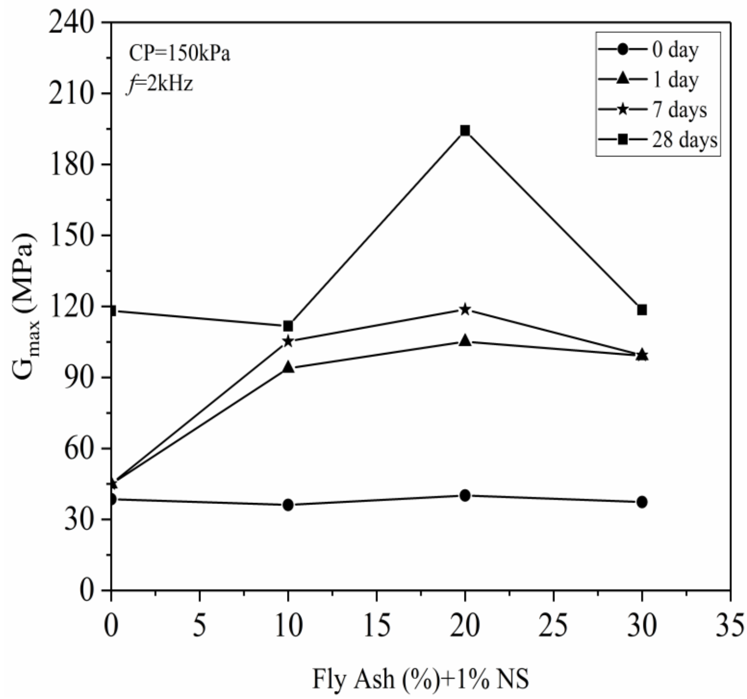

(f)

Fig. 7.7. Variation of G_{max} with fly ash and 1% Nano-SiO_2 (NS) content for variable (e) CP=150kPa, *f*=1kPa, and (f) CP=150, *f*=2kHz.

Table 7.1. Summary of bender element tests performed for both treated and untreated soil under different confining pressure.

Category	*f* (kHz)	CP (kPa)	Time lag, Δt(μs)	Shear wave velocity, Vs (m/s)	Shear modulus, G_{max} (MPa)
Clay	1	0	880	90.9	15.56
Clay	1	50	740	108.1	22
Clay	1	100	700	114.28	24.6
Clay	1	150	660	121.21	27.66
Clay	2	0	720	111.11	23.24
Clay	2	50	650	123	28.52
Clay	2	100	610	131.14	32.38
Clay	2	150	590	135.6	34.61
Clay+1%NS	1	0	460	193.91	57.17
Clay+1%NS	1	50	440	181.81	62.49
Clay+1%NS	1	100	420	190.47	68.58
Clay+1%NS	1	150	400	200	75.61
Clay+1%NS	2	0	360	222.22	93.35
Clay+1%NS	2	50	350	228.57	98.76
Clay+1%NS	2	100	340	235.29	104.66
Clay+1%NS	2	150	320	250	118.15
Clay+1%NS+10%FA	1	0	480	166.67	52.81
Clay+1%NS+10%FA	1	50	420	190.47	68.97
Clay+1%NS+10%FA	1	100	390	205.13	79.99
Clay+1%NS+10%FA	1	150	370	216.21	88.87
Clay+1%NS+10%FA	2	0	380	210.52	84.26
Clay+1%NS+10%FA	2	50	350	228.57	99.32
Clay+1%NS+10%FA	2	100	340	235.29	105.25
Clay+1%NS+10%FA	2	150	330	242.42	111.73
Clay+1%NS+20%FA	1	0	340	235.29	105.05
Clay+1%NS+20%FA	1	50	340	235.29	105.05
Clay+1%NS+20%FA	1	100	300	266.67	134.94
Clay+1%NS+20%FA	1	150	280	285.71	154.9
Clay+1%NS+20%FA	2	0	300	266.67	134.94
Clay+1%NS+20%FA	2	50	290	275.86	144.4
Clay+1%NS+20%FA	2	100	270	296.29	166.59
Clay+1%NS+20%FA	2	150	250	320	194.31
Clay+1%NS+30%FA	1	0	420	190.47	68.82
Clay+1%NS+30%FA	1	50	420	190.47	68.82
Clay+1%NS+30%FA	1	100	400	200	75.88
Clay+1%NS+30%FA	1	150	380	210.52	84.08

Category	f (kHz)	CP (kPa)	Time lag, Δt(μs)	Shear wave velocity, Vs (m/s)	Shear modulus, G_{max} (MPa)
Clay+1%NS+30%FA	2	0	360	222.22	93.68
Clay+1%NS+30%FA	2	50	340	235.29	105.02
Clay+1%NS +30%FA	2	100	340	235.29	105.02
Clay+1%NS+30%FA	2	150	320	250	118.57

7.4 COMPARISON OF SMALL-STRAIN SHEAR MODULUS (G_{max}) OF THE UNTREATED AND TREATED SOIL

A few results have been reported on the G_{max} of clayey soil treated with Nano-SiO_2. Fig. 7.8 illustrates the comparison of the small-strain shear modulus of the clayey soil treated with Nano-SiO_2 in the past and present studies. The small-strain shear modulus (G_{max}) value was increased to 270% with the inclusion of 1% Nano-SiO_2 and 7% lime at 28 days of curing for CL soil (Jafari et al. 2021). The G_{max} value of CL soil increased to about 153.54% with 15% cement and 1% Nano-SiO_2 (Heidarizadeh et al. 2021). The small-strain shear modulus (G_{max}) was increased to about 220.8% with the inclusion of 1% Nano-SiO_2 and 1% cement of high plastic (CH) soil (Thomas and Rangaswamy 2022). In the current study, the small-strain shear modulus (G_{max}) was increased to about 461.3% with the inclusion of 1% Nano-SiO_2 and 20% fly ash at 28 days of curing for CH soil at the confining pressure of 150 kPa. The comparison concludes that Nano-SiO_2 alone has not shown effective results for the small-strain shear modulus (G_{max}) of present CH soil. However, Nano-SiO_2, along with other additives like fly ash, gives much more effective results for small-strain shear modulus (G_{max}) of CH-type soils.

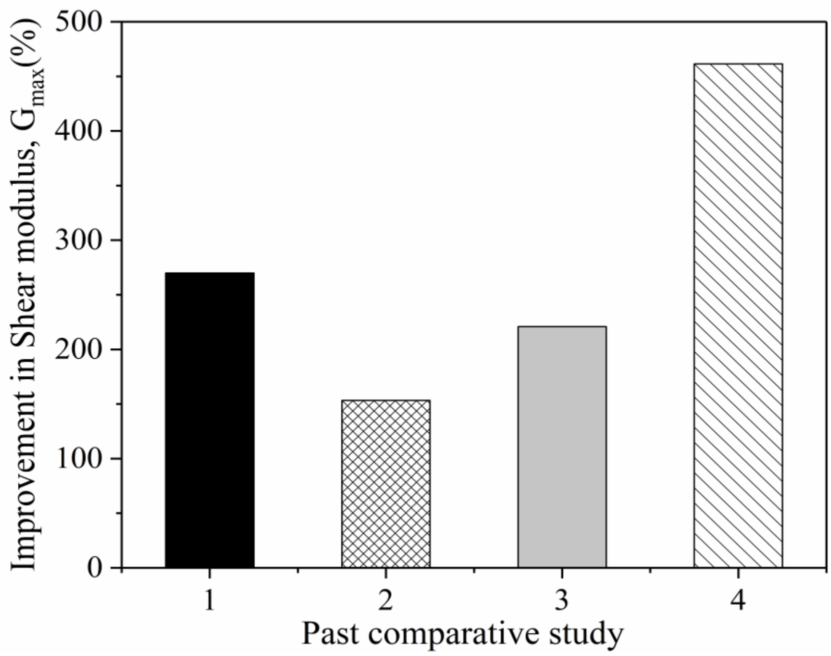

Fig. 7.8. Comparisons of improvement in small-strain shear modulus (G_{max}) with Nano-SiO_2 and other additives at 28 days curing. (1. Jafari et al. 2021, 2. Heidarizadeh et al. 2021, 3. Thomas and Rangaswamy 2022, 4. Present study)

7.5 CORRELATION BETWEEN SMALL-STRAIN SHEAR MODULUS (G_{max}) AND SHEAR STRENGTH (τ)

The relationship between the small-strain shear modulus with other geotechnical properties can be developed using mathematical equations to implement it in seismic response analysis. To develop a correlation between the G_{max} and shear strength (τ) of the current soil matrix, a series of triaxial tests were conducted on the treated soil samples for curing ages of 0, 1, 7, 14, and 28 days with various fly ash concentrations and 1% Nano-SiO_2 at an axial loading rate of 1.2 mm/min. Fig.7.9 depicts the variation of G_{max} and shear strength (τ) for the treated soil samples on various curing days. From the figure, it can be observed that the samples are split into two test groups. The samples in the first group were treated with 1% Nano-SiO_2, whereas the samples in the second group were treated with 1% Nano-SiO_2 and different fly ash contents (10%, 20%, and 30%) at various confining pressures. The results demonstrated that as curing time increases, the effect of Nano-SiO_2 and fly ash tends to increase the specimen's shear strength and small-strain shear modulus. The best-fit curve for the obtained results using a power equation established an acceptable correlation between the small-strain shear modulus (G_{max}) and shear strength (τ) of the treated soil. The developed relationship can be used to estimate the G_{max} of the specimens from the triaxial test results using the following mathematical equation (Eq. 7.1).

$$G_{max} = 0.027\tau^{1.305} \tag{7.1}$$

Here, G_{max} (small-strain shear modulus) and τ (shear strength) are expressed in MPa and kPa respectively.

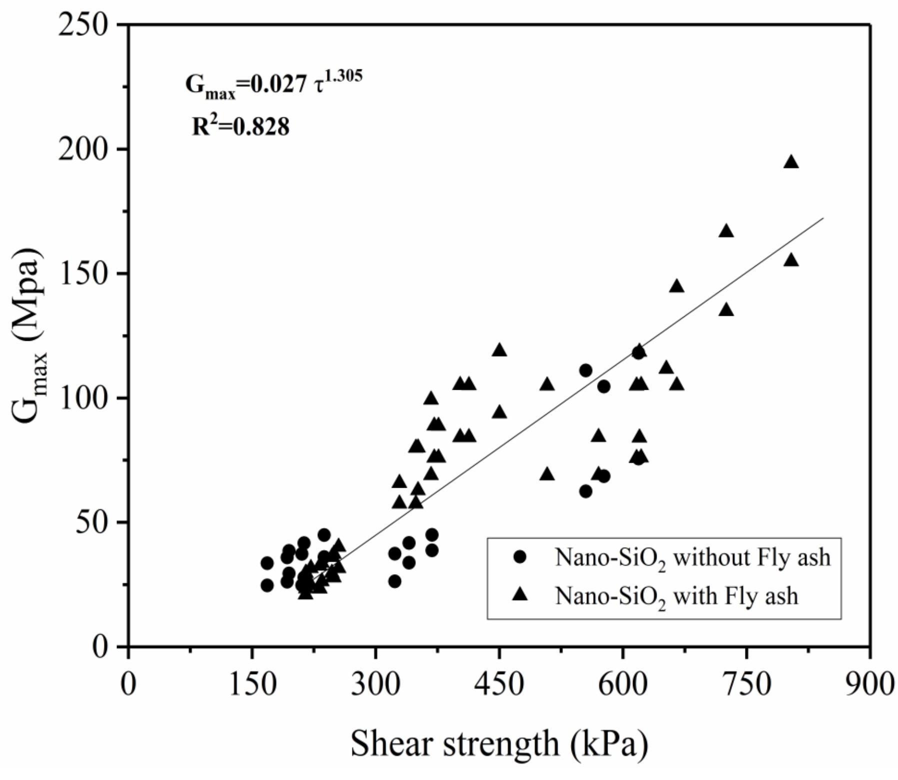

Fig. 7.9. Correlation between small-strain shear modulus (G_{max}) and shear strength (τ) of clayey soil treated with fly ash and Nano-SiO_2.

7.6 ASSESSMENT OF NORMALIZED SHEAR MODULUS AND MODEL FITTING FOR THE UNTREATED AND TREATED SOIL

The well-known investigations by Hardin and Black (1968) and (1969) and Hardin and Drnevich 1972 (a) and 1972 (b) established the empirical equations to measure the dynamic modulus reduction and damping ratio curve for clayey soil. Furthermore, many investigators have employed hyperbolic models to explain the nonlinear behaviour of soils under various cyclic loading conditions (Kondner 1963; Duncan and Chang 1970; Darendeli 2001; Vardanega 2013). The current study attempted to establish empirical relationships between the normalized modulus reduction (G/G_{max}) and shear strain (γ) of the clay, the optimized Nano-SiO_2 treated soil, and the optimized Nano-SiO_2 and fly ash treated soil. The correlations developed between the G/G_{max} and the γ of clay soil, optimized Nano-SiO_2 treated soil, and optimized Nano-SiO_2 and fly ash treated soil are presented in Eq. 7.2, 7.3 and 7.4 respectively.

$$G/G_{max} = 0.138- 0.042\,\gamma \quad (R^2=0.81) \tag{7.2}$$

$$G/G_{max} = 0.178- 0.054\,\gamma \quad (R^2=0.94) \tag{7.3}$$

$$G/G_{max} = 0.149 - 0.04\,\gamma \quad (R^2=0.84) \tag{7.4}$$

The experimental results reported by Hardin and Drnevich 1972 (a) and 1972 (b), Stokoe et al. (1999) suggested a hyperbolic relationship between the normalized shear modulus ratio (G/G_{max}) and cyclic shear strain (γ). Here, an attempt has been made to develop similar hyperbolic relationship for the clay soil, optimized Nano-SiO_2 treated soil, and optimized Nano-SiO_2 and fly ash treated soil. The correlations between normalized shear modulus ratio (G/G_{max}) with cyclic shear strain (γ) for the clay soil, optimized Nano-SiO_2 treated soil, and optimized Nano-SiO_2 and fly ash treated soil were fitted to a hyperbolic model taking γ as an independent variable, and G/G_{max} as dependent variables and expressed in Eq.7.5. Fig. 7.10 (a) ; Fig. 7.11 (b) and (c); Fig. 7.12 (d) and (e) depicts the variation of normalized modulus reduction/ normalized shear modulus ratio (G/G_{max}) with the cyclic shear strain of the untreated and treated samples. The value of curves fitting parameters a, b, and R^2 of the fitted normalized shear modulus ratio (G/G_{max}) with cyclic shear strain (γ) curve are about 0.124, 1.13, and 0.99; 0.079-0.124, 1-1.19, and 0.93-0.98; and 0.082-0.12, 1.066-1.327, and 0.97-0.98 for clay soil, optimized Nano-SiO_2 treated soil, and optimized Nano-SiO_2 and fly ash treated soil respectively (Table 7.2).

$$\frac{G}{G_{max}} = \frac{1}{1+\left(\frac{\gamma}{a}\right)^{b}} \tag{7.5}$$

where, G/G_{max}: normalized shear modulus ratio, γ: cyclic shear strain, and a & b are curve fitting parameters.

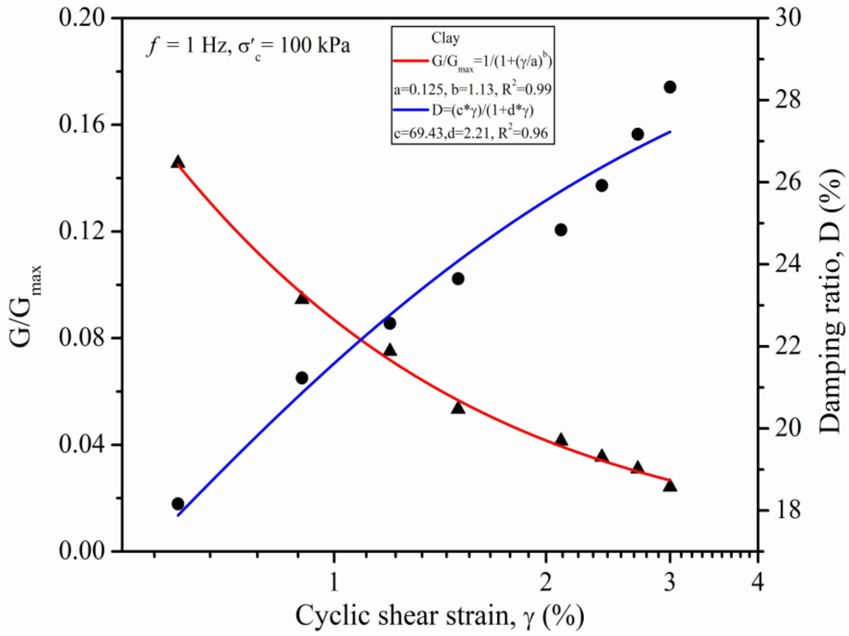

(a)

Fig. 7.10. Variation of normalized shear modulus ratio and damping ratio with cyclic shear strain (a) Clay.

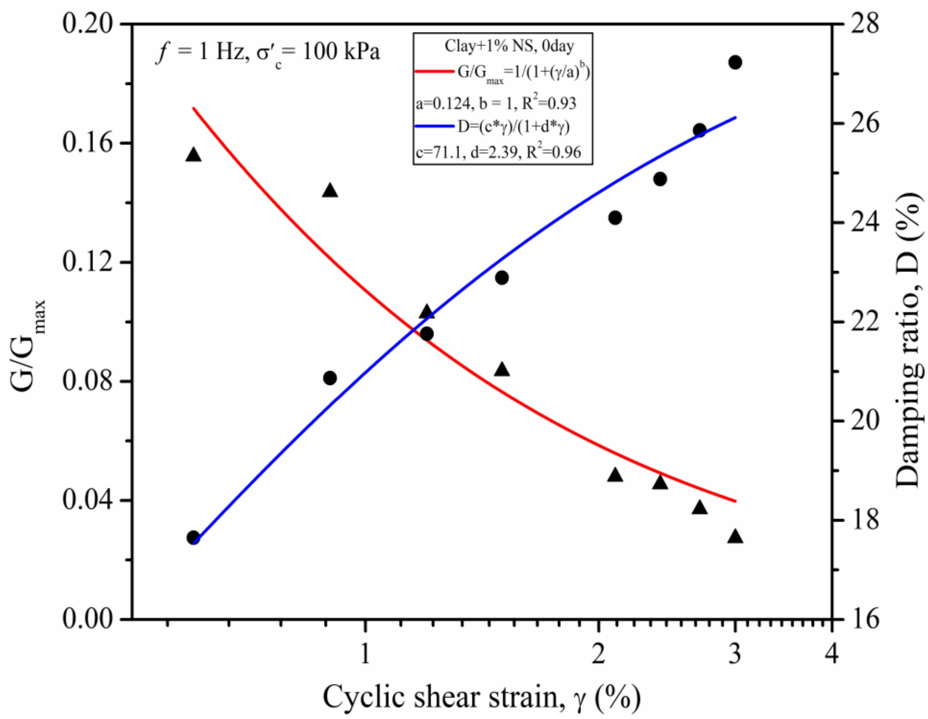

(b)

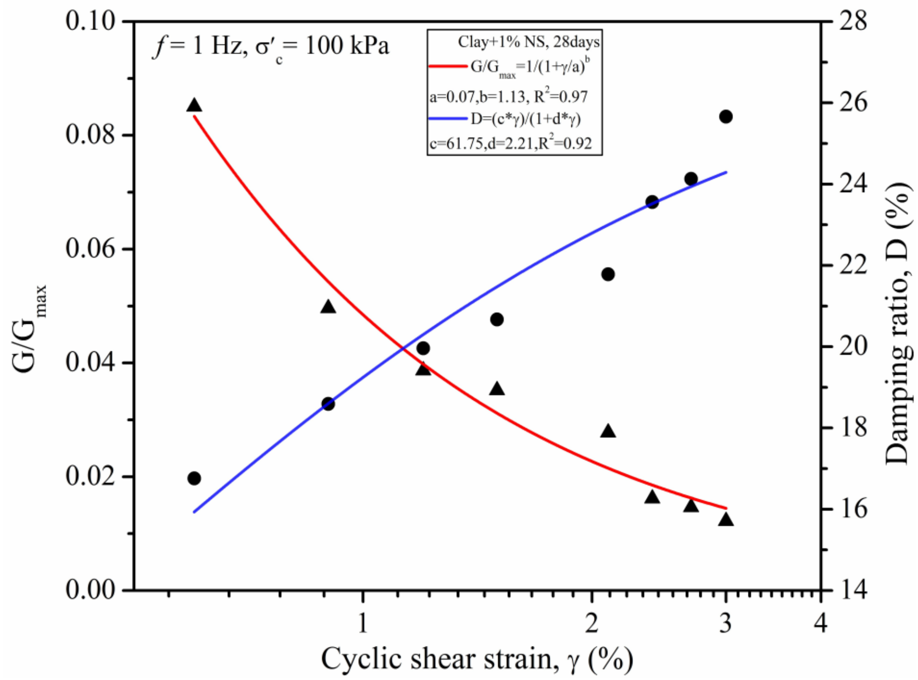

(c)

Fig. 7.11. Variation of normalized shear modulus ratio and damping ratio with cyclic shear strain (b) Clay+1%NS, 0day, (c) Clay+1%NS, 28days.

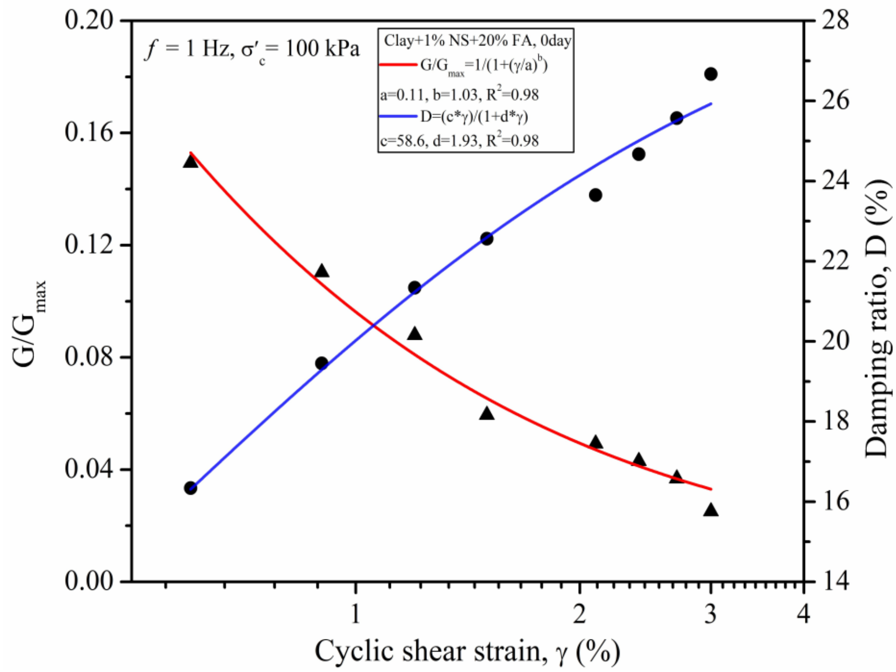

(d)

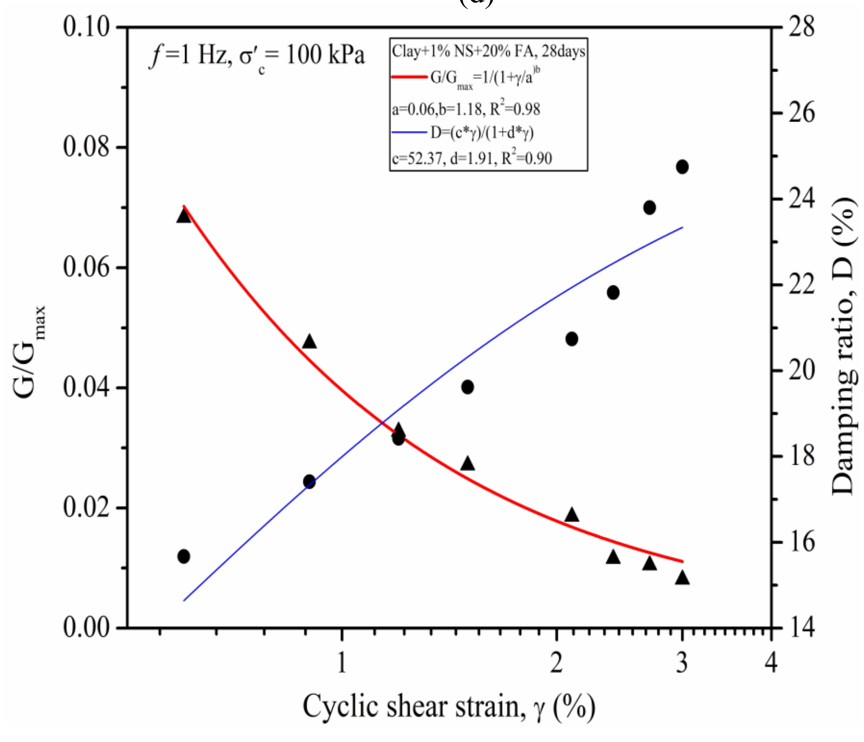

(e)

Fig. 7.12. Variation of normalized shear modulus ratio and damping ratio with cyclic (d) Clay+1%NS+20%FA, 0day, and (e) Clay+1%NS+20%FA, 28days.

Table 7.2. Variation of curve fitting parameters of normalized modulus reduction curves.

SL No.	Combinations	Curing period (days)	G/G_{max}		
			a	b	R^2
1	Clay	0	0.125	1.13	0.99
2	Clay+1%NS	0	0.124	1	0.93
3	Clay+1%NS	28	0.07	1.13	0.97
4	Clay+1%NS+20%FA	0	0.11	1.03	0.98
5	Clay+1%NS+20%FA	28	0.06	1.18	0.98

7.7 ASSESSMENT OF DAMPING RATIO AND MODEL FITTING FOR THE UNTREATED AND TREATED SOIL

Here, an attempt has also been made to develop a relationship between D and γ for the present clay soil, optimal content of Nano-SiO_2 treated soil, and optimal content of Nano-SiO_2 and fly ash treated soil. The correlations between damping ratio (D) and cyclic shear strain (γ) for the present clay soil, optimal content of Nano-SiO_2 treated soil, and optimal content of Nano-SiO_2 and fly ash treated soil were fitted to a hyperbolic model by taking γ as an independent variable, and the damping ratio as a dependent variables and expressed in Eq. 7.6.

$$D = (c \times \gamma)/(1 + d \times \gamma) \tag{7.6}$$

where, D: damping ratio, γ: cyclic shear strain, and c & d are curve fitting parameters. Fig. 7.6 depicts the response of D with a cyclic shear strain of the untreated and treated samples. Table 7.3 illustrates the values of the curve fitting parameters c, d, and R^2 of the untreated and treated samples. The differentiated node-point analysis was based on variations in nano-silica and fly ash proportions across soil samples, and a logic tree framework was introduced to evaluate different sampling strategies systematically. Each branch of the logic tree represents a combination of mixture proportions and testing conditions, with assigned weights based on performance criteria such as strength gain, durability, and rheological behaviour (Güllü and İyisan 2016). This method aligns with where ground motion prediction models are compared using weighted logic trees. Analogously, we apply logic tree weighting to select the most promising soil-nano silica-fly ash mixture, offering a probabilistic basis for experimental optimization.

Table 7.3. Variation of curve fitting parameters of damping ratio curves.

SL No.	Combinations	Curing period (days)	D		
			c	d	R^2
1	Clay	0	69.43	2.21	0.96
2	Clay+1%NS	0	71.1	2.39	0.96
3	Clay+1%NS	28	61.75	2.21	0.92
4	Clay+1%NS+20%FA	0	58.6	1.93	0.98
5	Clay+1%NS+20%FA	28	52.37	1.91	0.90

7.8 COMPARISON OF NORMALIZED SHEAR MODULUS RATIO WITH PAST LITERATURE

Since the early 1970s, research on modulus reduction relationships for clays has been conducted worldwide. Throughout the past two decades, the hyperbolic model has been extensively used to characterize the relationship between the G/G_{max} and γ in the non-linear range. The G_{max} at low strain is evaluated from the BE test. In the current study, the normalized modulus reduction curve with γ is plotted in Fig. 7.13 alongside the findings of the other researchers. The normalized shear modulus initially decreased slowly and then decayed rapidly. According to Vucetic and Dobry (1991), the plasticity index (I_p) is an important parameter in determining the dynamic modulus of both normally consolidated and over-consolidated soils. The G/G_{max} increased with the rise in Ip. The response curve for soil with I_p values of 15 and 30 is displayed in Fig. 7.7. Thomas and Rangaswamy 2020 demonstrated the normalized shear modulus response curve of the untreated and treated soil with I_p of 58 and 16.5, respectively. According to the findings, the response curve shifted upward for I_p of 58 and somewhat downward for I_p of 16.5. By comparing the curves, it is clear that the G/G_{max} of the current study falls within the boundary range of the previously reported results.

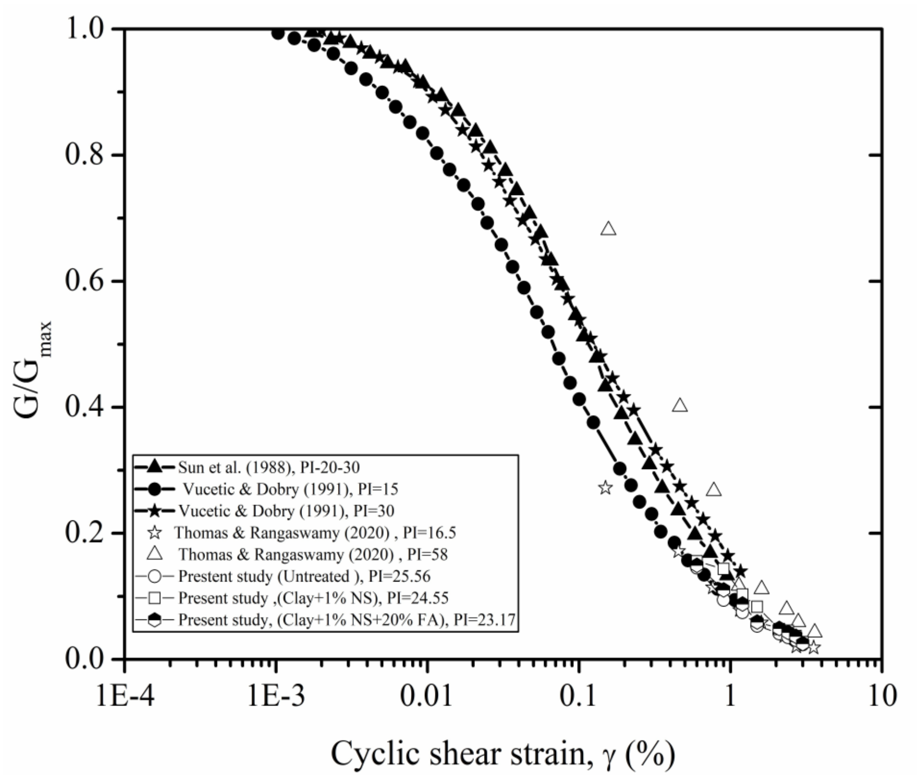

Fig. 7.13. Comparison of normalized shear modulus ratio with cyclic shear strain of the untreated and treated soil with past studies.

7.9 COMPARISON OF DAMPING RATIO WITH PAST LITERATURE

The damping ratio is the key element for determining the energy absorption capabilities of the soil. It is widely acknowledged that the material damping ratio of soil depends on the shear strain. In the present study, the damping ratio of soil with cyclic strain is compared with the other researchers for different I_p (Fig. 7.14). In comparison to soils with a lower I_p, those with higher plasticity typically exhibit a more linear cyclic stress-strain response at small strains and deteriorate less at larger shear strain. A higher damping ratio was observed for a low I_p of 15 and a lower value for a high I_p of 30 (Vucetic et al. 1991). Similarly, virgin soil with a high plasticity Ip had a low D value, whereas treated soil with a low Ip of 16.5 had a high D value and was found to have increased D with increased cyclic strain (Thomas and Rangaswamy 2020). The damping ratio in the current investigation is within the range of the findings from earlier research.

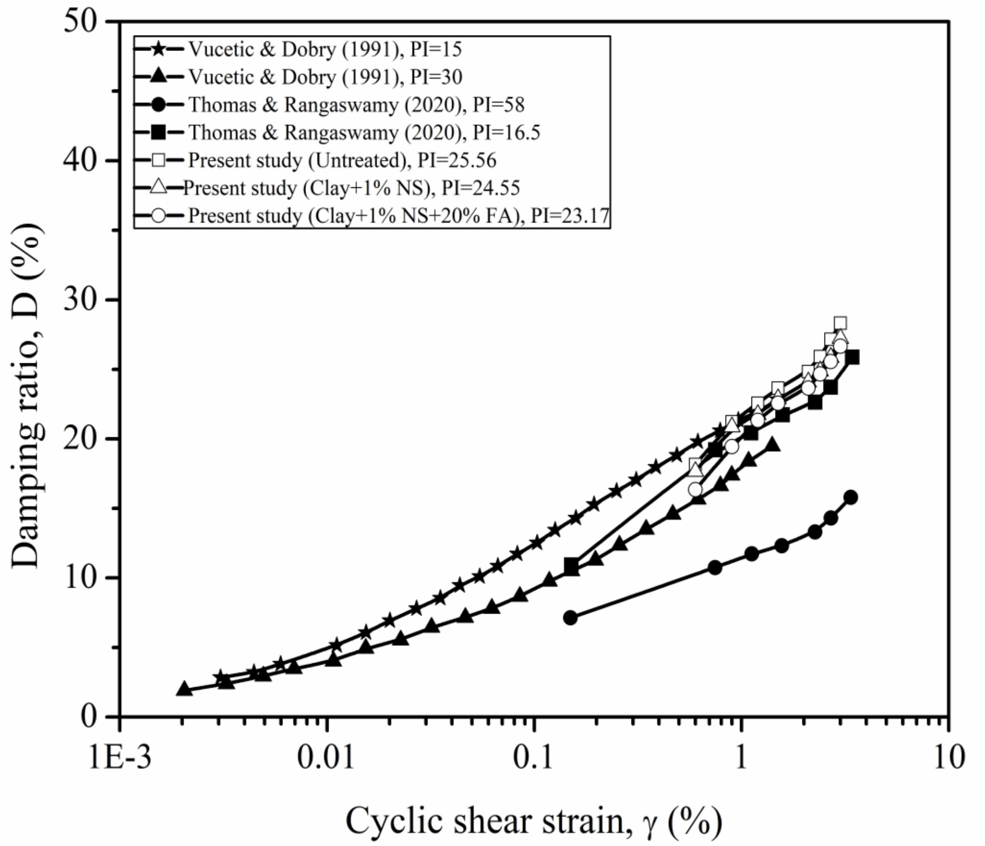

Fig. 7.14. Comparison of damping ratio with cyclic shear strain of the untreated and treated soil with past studies.

7.10 SUMMARY

This chapter discussed about the evaluation of small-strain shear modulus (G_{max}) of the untreated and treated clayey soil, and its normalization with high-strain dynamic shear modulus. Also, the models were fitted to the present generated normalized data of the untreated and treated soil. In addition, a correlation between the G_{max} and shear strength (τ) of the treated clayey soil has also been developed. The following conclusions can be drawn from the above-mentioned experimental and correlation analysis.

The results of the study show that G_{max} grows proportionally to confining pressure, input wave frequency, and these factors have a direct association with each other. The G_{max} increased higher than the untreated soil for 28 days curing period. Stabilization results in a stiffer and denser soil matrix; the treated soil has a greater V_s value than that of the parent soil. Empirical relationships between the G/G_{max} versus γ and D versus γ of the clay, the optimized Nano-SiO_2 treated soil, and the optimized Nano-SiO_2 and fly ash treated soil were established. The developed G/G_{max} and damping ratio curves fit the database well. The results can be useful for predicting the seismic behaviour of the Nano-SiO_2 and fly ash-treated clayey soil under various strain conditions.